Supporting Information for

Dye-Induced Photoluminescence Quenching of Quantum Dots: Role of Excited State Lifetime and Confinement of Charge Carriers

Saleem Al-Maskari[1], Abey Issac[1,*], Srinivasa Rao Varanasi [1], Richard Hildner[2], R.G. Sumesh Sofin[1], A. Ramadan Ibrahim[3], Osama K. Abou-Zied[3]

1 Department of Physics, College of Science, Sultan Qaboos University, Muscat 123, OMAN

2 Zernike Institute for Advanced Materials, University of Groningen, Nijenborgh 4, 9747 AG

Groningen, The Netherlands

3 Department of Chemistry, College of Science, Sultan Qaboos University, Muscat 123, OMAN

*E-mails: "Abey Issac" abeyissac@squ.edu.om

1. Femtosecond transient absorption measurements

The ultrafast transient absorption measurements were performed using a femtosecond laser setup that was previously described in detail [6]. Briefly, pump and probe pulses were obtained using a regenerative amplified Ti:Sapphire laser (Libra, Coherent). The Libra generates compressed laser pulses (70 fs pulse width) with output of 4.26 W at a repetition rate of 5 kHz and centered at 800 nm. The output beam was split into two parts. The major portion of the output pulse was used to pump a Coherent OPerA Solo (Light Conversion Ltd.) optical parametric amplifier to generate spectrally tunable light spanning the range 240–2600 nm and is used as the pump beam. The remaining small portion of the laser output was focused on a sapphire crystal to generate a white light continuum in the range 430-800 nm which is used as the probe beam in a Helios transient absorption spectrometer (Ultrafast Systems, LLC). The probe light was measured by a fiber optic that is coupled to a multichannel spectrometer with a CMOS sensor in the range 350-850 nm. Chirp in the white light continuum probe was minimized by using parabolic mirrors. Rotational contribution to the overall excited state decay kinetics was removed by depolarizing the pump beam using a depolarizer (DPU-25, Thorlabs). The pump pulse was attenuated to ~100 nJ in order to avoid multiphoton excitation. The pump and probe pulses were focused on the sample and the temporal delay of the probe pulse was varied using a computer-controlled optical delay

stage. Kinetic traces at appropriate wavelengths were assembled from the time-resolved spectral data. Surface Xplorer software (supplied by Ultrafast Systems) was used for data analysis. The IRF was measured from Raman scattering to be ~ 120 fs. The samples were prepared in 2 mm fused silica cuvettes (Starna Scientific) and were stirred during the experiment to avoid photodegradation. In order to adjust the zero delay for each wavelength and to get the chirp-corrected spectrum, we carried out the transformation process using the software program (Surface Xplore).

2. Determination of the dye-to-QD concentration ratio [x]

The Beer-Lambert law provides the concentration of a solution by measuring its absorbance. The linear relationship between the concentration and the absorbance of the solution is given by the equation [1];

$$Absorbance\ (OD) = \varepsilon(\lambda)\, l\, C \qquad (1)$$

where ε is the extinction coefficient (expressed in L $mol^{-1}cm^{-1}$) for a specific wavelength, l is the optical path length (in cm) and c is the concentration in mol L^{-1}. The dye-to-QD concentration ratio [x] is determined using equation 2;

$$[X] = \frac{\mathrm{C_{Dye}}}{\mathrm{C_{QD}}} \qquad (2)$$

where

$$C_{\mathrm{Dye}} = \frac{OD_{Dye\ in\ the\ assembly}}{\varepsilon_{Dye} l} \qquad (3)$$

$$\mathrm{C_{QD}} = \frac{OD_{QD}}{\varepsilon_{QD} l} \qquad (4)$$

Therefore;

$$[X] = \frac{OD_{Dye\ in\ the\ assembly} \cdot \varepsilon_{QD}}{\varepsilon_{Dye} \cdot OD_{QD}} \qquad (5)$$

Table S1: Concentration of the quencher molecule $[Q]$ and the corresponding dye-to-QD molar ratio $[X]$ for different QD-dye assemblies. Following extinction coefficients are used; CIS QDs: $4.12 \times 10^5\ M^{-1}\ cm^{-1}$ at 400 nm, InP QDs: $2.6\times 10^5\ M^{-1}\ cm^{-1}$ at 548 nm, Rh575: $9.7 \times 10^4\ M^{-1}cm^{-1}$ at 518 nm and Rh560: $7 \times 10^4\ M^{-1}cm^{-1}$ at 500 nm [2-4]

Assembly	$[Q]\ \mu mol/L$	$[X]$	Assembly	$[Q]\ \mu mol/L$	$[X]$
CIS-Rh575	0.01	0.1	CIS-Rh560	0.05	0.3
	0.05	0.5		0.13	0.8
	0.08	0.8		0.20	1.2
	0.12	1.2		0.43	2.6
	0.16	1.6		0.71	4.3
	0.20	2.0		0.89	5.3
	0.34	3.4		1.10	6.6
	0.44	4.4		1.30	7.8
	0.63	6.3		1.60	9.6
	0.69	6.9		1.90	11.4
	0.75	7.5		2.10	12.6
				2.80	16.8
InP-Rh575	0.83	2.7	InP-Rh560	0.26	0.9
	1.60	5.2		1.05	3.5
	1.94	6.3		1.30	4.4
	3.02	9.8		2.23	7.5
	3.14	10.2		3.09	10.3
	3.88	12.6		4.63	15.5
	4.19	13.6		5.73	19.6
	4.59	14.9		7.19	24.1
	5.28	17.2			
	10.26	33.3			

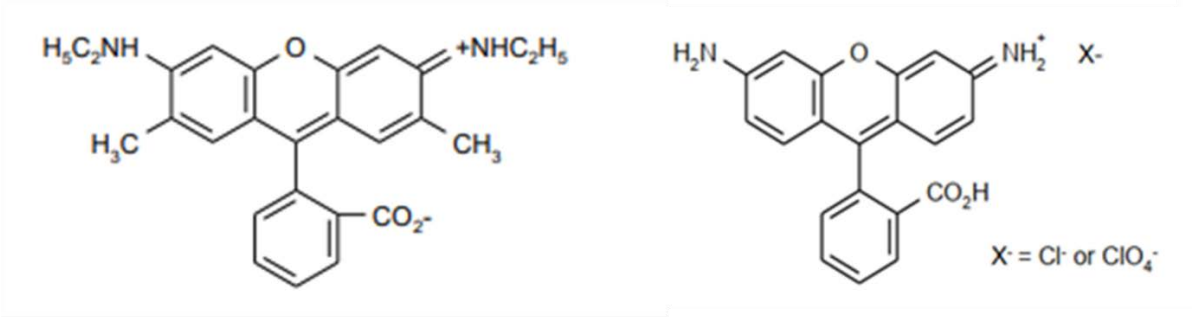

Rh575 **Rh560**

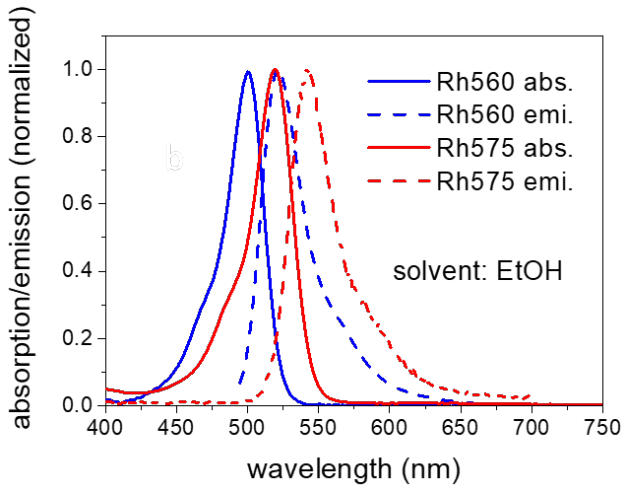

Figure S1: Molecular structures of Rh575 and Rh560 dye molecules (top) and their absorption and emission spectra in ethanol (bottom).

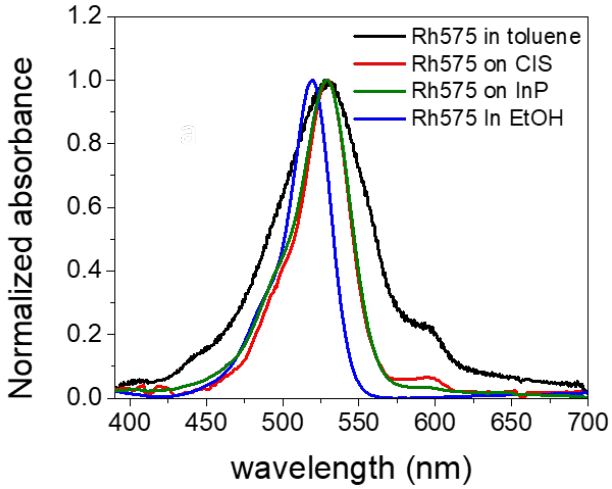

Figure S2: Absorption spectra of Rh575 in different environments. The spectrum on QD surface is obtained by subtracting QD spectrum from the QD-dye spectrum.

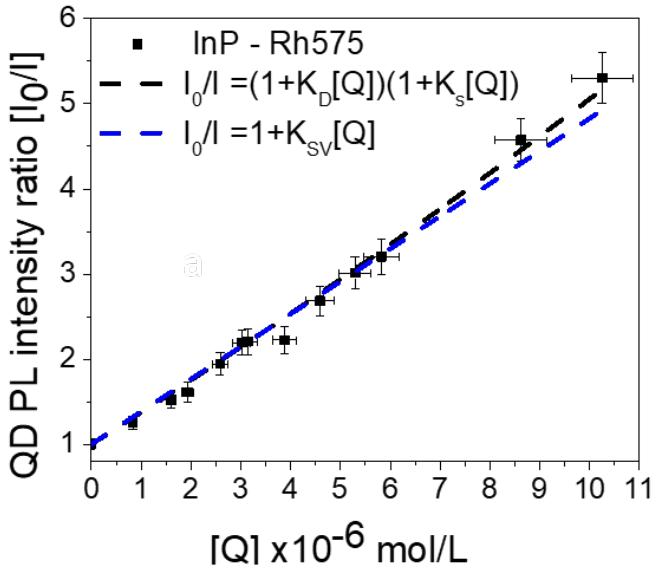

Figure S3: Comparison of quadratic (black dashed line) and linear (blue dashed line) forms of Stern-Volmer equations fitted to the I_0/I vs. [Q] data.

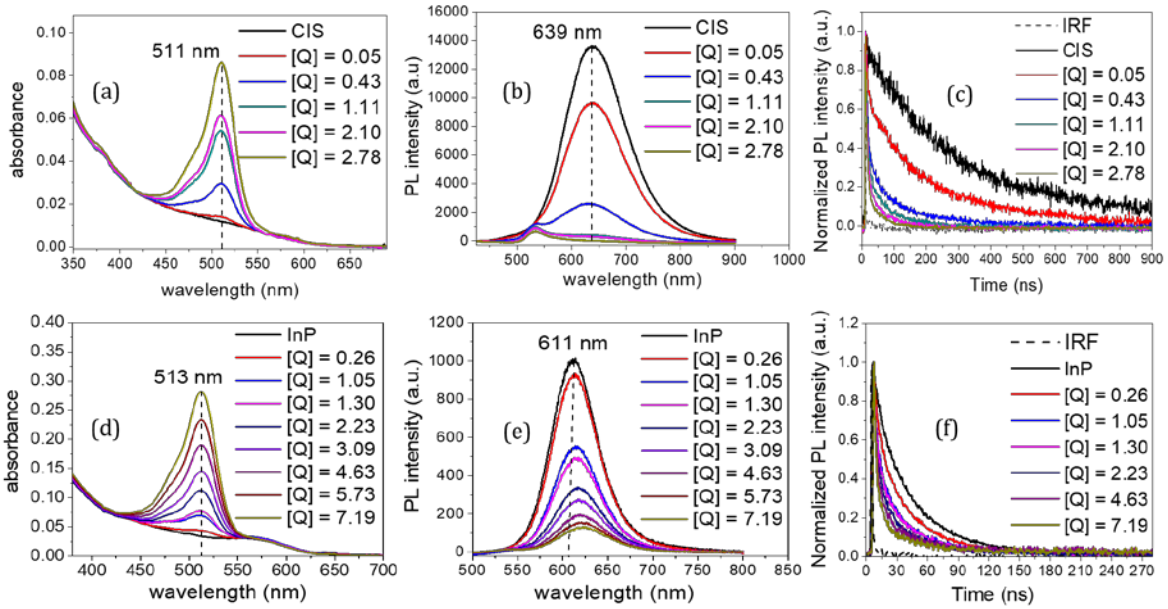

Figure S4: Absorption, emission spectra and emission decay transients of CIS-Rh560 (a-c) and InP-Rh560 (d-f) assemblies in toluene. The legend [Q] is the molar concentration of Rh560 in μmol/L. λ_{ex} = 410 nm. Figures a-c adopted from [5].

3. Förster resonant energy transfer (FRET) efficiency calculation

According to FRET theory, the energy transfer efficiency E_{ET}^{r} is given by equation;

$$E_{ET}^{r} = \frac{1}{1 + \left(\frac{r}{R_0}\right)^6} \qquad (6)$$

Here, r is the distance between the center-of-mass of donor (QD) and acceptor (dye), which we estimate to r = 3.45 nm for the CIS-dye assemblies and to r = 3.05 nm for the InP-dye assemblies. The Föster radius R_0 is given by the equation;

$$R_0 = 0.2018 \left(\frac{\emptyset_D \, k^2 \, J(\lambda)}{n^4}\right)^{\frac{1}{6}} \qquad (7)$$

where $\emptyset_D$ is the quantum yield of the donor in the absence of the acceptor, k is the orientation factor describing the relative orientations of the transition dipoles of the donor and acceptor (here we use the orientational average, i.e., $k^2 = 2/3$), $J(\lambda)$ is the spectral overlap integral between the normalized donor emission and acceptor absorption, and n is the refractive index of the medium (taken here as the refractive index of the ZnS shell, n = 2.4). The efficiency of energy transfer E_{ET}^{r}, i.e., the fraction of photons absorbed by the donor which are transferred non-radiatively to the acceptor, is then compared to the quenching efficiencies that are calculated using the lifetime (E_q^{τ}) and the emission intensity (E_q^{I}) data (see Figs. 1c, 2b, 3c, 4b, S4) as;

$$E_q^{\tau} = 1 - \frac{\tau}{\tau_0} \qquad (8)$$

$$E_q^{I} = 1 - \frac{I}{I_0} \qquad (9)$$

respectively. In Table S2 we provide for illustration the values for all efficiencies for a dye-to-QD ratio of 1.

Table S2: Estimated values of the spectral overlap integral J, Föster radius R_0, and the efficiency of energy transfer E_{ET}^r as well as the quenching efficiencies E_q^τ and E_q^I.

System	τ_0 (ns)	$\emptyset_D$	$J \times 10^{13}$ $(nm^4M^{-1}cm^{-1})$	R_0 (nm)	r (nm)	E_{ET}^r (%)	E_q^τ (%)	E_q^I (%)
CIS-Rh560	290	0.4	9.236	1.92	3.45	2.9	62	66
InP-Rh560	37	0.2	2.067	1.33	3.05	0.7	18	18
CIS-Rh575	290	0.4	39.98	2.45	3.45	11.4	71	79
InP-Rh575	37	0.2	18.86	1.93	3.05	6.0	16	18

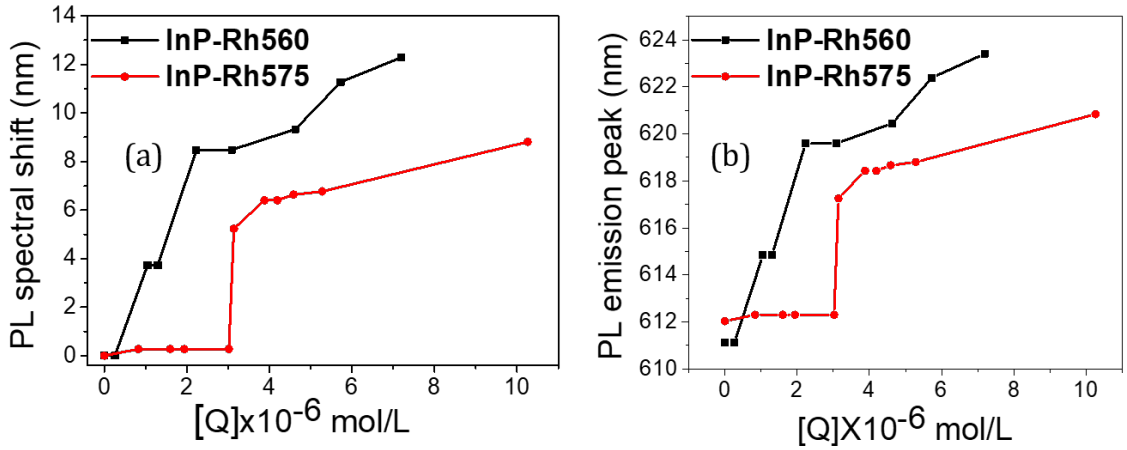

Figure S5: (a) PL spectral shift and (b) peak emission wavelength of InP QDs forming assemblies with Rh560 (black) and Rh575 (red) dye molecules in toluene.

References

1. Valeur, B., Molecular Fluorescence: Principles And Applications, 2nd, Wiley-VCH, 2001.
2. Xia, C., et al., Size-Dependent Band-Gap and Molar Absorption Coefficients of Colloidal $CuInS_2$ Quantum Dots. ACS Nano, 2018. 12(8): p. 8350-8361.
3. Brackmann, U., Lambdachrome®Laser Dyes. Lambda Physik AG, Germany, 2000 (3rd Edition).
4. Thomas, A., et al., How Trap States Affect Charge Carrier Dynamics of CdSe and InP Quantum Dots: Visualization through Complexation with Viologen. ACS Energy Letters, 2018. 3(10), 2368-2375
5. Issac, A., et al., Photoexcited Charge Trapping Induced Quenching of Radiative Recombination Pathways in $CuInS_2$/ZnS-Dye Nanoassemblies. Journal of Luminescence, 2021, 239, 118402
6. Ibrahim, I.; Lim, H. N.; Abou-Zied, O. K.; Huang, N. M.; Estrela, P.; Pandikumar, A. Cadmium Sulfide Nanoparticles Decorated with Au Quantum Dots as Ultrasensitive Photoelectrochemical Sensor for Selective Detection of Copper(II) Ions. The Journal of Physical Chemistry C 2016, 120, (39), 22202-22214